Correspondence
https://doi.org/10.1631/jzus.B2600040

Infra-slow body-surface potentials show a group-level association with thyroid cancer

Bohan DENG[1,3], Ruili ZHANG[4], Yuxuan LIU[1], Jinglao LIN[1], Shicong GUI[1], Xihao WEI[1], Yin CHENG[4], Li ZHENG[4], Shaohua HU[4], Pingping LYU[4], Yubo LI[1,2,3], Huafen WANG[4]

[1]*College of Information Science and Electronic Engineering, Zhejiang University, Hangzhou 310027, China*
[2]*Zhejiang Key Laboratory of Intelligent Rehabilitation and Translational Neuroelectronics, Hangzhou 310027, China*
[3]*International Joint Innovation Center, Zhejiang University, Haining 314400, China*
[4]*The First Affiliated Hospital of Zhejiang University School of Medicine, Hangzhou 310003, China*

Thyroid cancer is a common malignancy with broad systemic endocrine and metabolic effects (Hammond et al., 2024). Regarding diagnostics, if infra-slow body-surface potential (BSP) features reflect a systemic state, then this type of cancer is a reasonable clinical test case. Prior electrodermal work has focused on faster transients above 0.5 Hz (Boucsein, 2012; Posada-Quintero and Chon, 2020), and task-state skin potential abnormalities have been shown to distinguish mood disorders from healthy controls (Lyu et al., 2024). We concentrated on an infra-slow band from 0.025 to 0.2 Hz, called Band 1 herein. We evaluated whether infra-slow features carry reproducible group-level information when artifacts are explicitly controlled, with one pre-specified primary endpoint. "Separable" here means a group-level statistical difference, not individual-level diagnosis. In a cohort of 321 cancer patients, Band 1 energy showed a clear group-level association with thyroid cancer, which persisted after automated QC and under stricter artifact-removal settings.

Unedited

✉ Yubo LI, lilinear@zju.edu.cn
Huafen WANG, 2185015@zju.edu.cn
Yubo LI, https://orcid.org/0000-0002-9135-8360
Huafen WANG, https://orcid.org/0000-0002-4674-4000
Bohan Deng, https://orcid.org/0009-0008-7523-0421

Received Jan. 22, 2026; Revision accepted Mar. 2, 2026;
Crosschecked xxx. xx, 20xx; Published online xxx. xx, 20xx

© Zhejiang University Press 2026

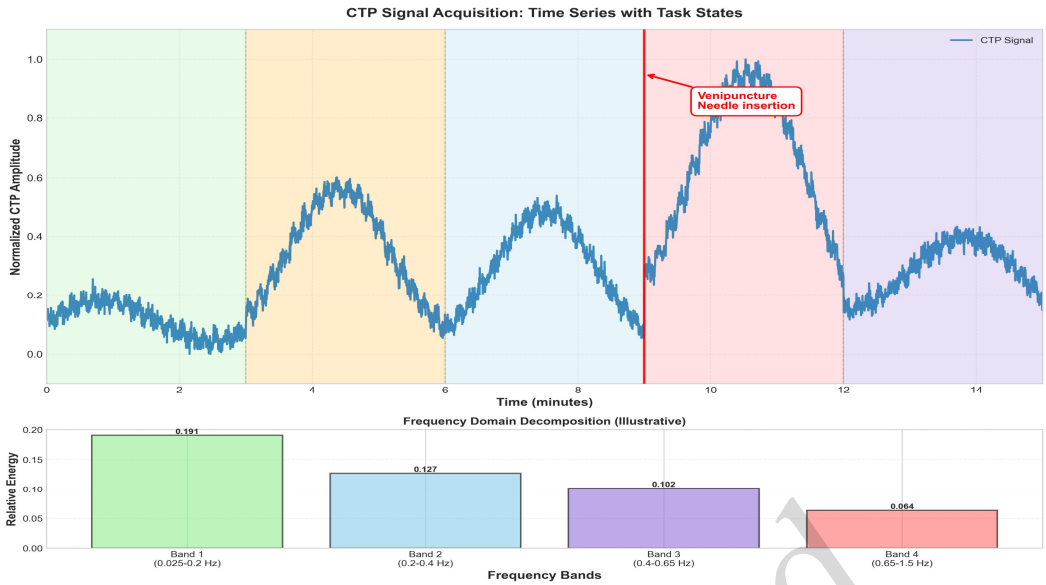

Fig. 1 Connective tissue potential (CTP) signal acquisition and frequency-domain decomposition. The upper panel shows a representative normalized CTP time series recorded across task states (color-coded background regions). The protocol includes resting, provocation, and recovery macro-phases. The red vertical line and annotation indicate the venipuncture needle-insertion event. Slow oscillations and sustained baseline shifts are preserved because a high-pass filter was not used. The lower panel shows the relative energy distribution across four frequency bands: Band 1 (0.025–0.2 Hz), Band 2 (0.2–0.4 Hz), Band 3 (0.4–0.65 Hz), and Band 4 (0.65–1.5 Hz), confirming that Band 1 contains the largest share of signal energy. Acquisition parameters: CTP008 amplifier, Zin > 100 MΩ, analog low-pass at 1.0 Hz, 5 Hz sampling, and no digital detrending.

Unedited

BSPs were recorded using a custom direct current (DC)-coupled system (CTP008). The input impedance was Zin > 100 MΩ, the input range was ±20 mV, and the common-mode rejection ratio (CMRR) was >100 dB. Equivalent input noise was <2.0 μV root mean square (RMS). Self-adhesive Ag/AgCl pads were placed on the right middle finger and inner wrist after alcohol-swab cleaning. The same sites were used for every participant because they are easy to access and support stable contact. Participants sat with the hand on the table and were told to stay still. The temperature in the rooms was between 22 and 25 °C. Sampling was performed at 5 Hz after a 1.0 Hz analog anti-aliasing filter. A digital high-pass filter and detrending were not applied. Preserving DC and infra-slow content was the central design choice. Each 15-minute session had three macro-phases: Resting, Provocation, and Recovery (Fig. 1). Provocation was split into three blocks—Positive, Neutral, and Negative—for analysis. The 321 patients involved were recruited under institutional ethical approval. Hardware and acquisition parameters are summarized in Supplementary Tables S1 and S2.

The clinical team reviewed all recordings for major problems, such as electrode detachment or non-compliance. All 321 sessions were retained for automated QC and feature extraction. Subsequently, three automated steps flagged segments within each recording. Clipping was flagged when voltage was constant (<0.01 mV change) for ⩾ 3 samples near the recording extremes. Step artifacts were flagged when the sample-to-sample jump exceeded 5 mV. Normal jumps were about 0.1 – 0.2 mV, which is far below this threshold. A ±1-sample guard was also used around each detected step. A motion surrogate was flagged when the local standard deviation (SD) in 10-s windows exceeded 5× the session median. On average, (3.0±8.5)% of each recording was excluded. For five participants, >40% of data were lost, and these participants were thus removed. The final analytic cohort was N=316. Two stricter threshold sets were also tested. For steps, the thresholds were >3 mV and >2 mV. For motion, the thresholds were >3× and >2× the session-median SD. The thyroid-cancer effect held and slightly strengthened ($p = 0.0038$, 0.0031, 0.0020; Supplementary Tables S3 and S4). Sensitivity reprocessing was based on raw-file estimation that required valid phase markers, so the per-threshold N can be slightly smaller than 316.

Band 1 energy is the Welch power spectral density (PSD) integral over 0.025–0.2 Hz per analysis block. A Hann window was employed with 120-s segments and 50% overlap. This yields one value per block and per person, and it reduces sensitivity to brief transients. Tonic baseline was the median DC voltage per block, referenced to the Resting block. A single primary endpoint was pre-specified as the Band 1 energy difference between thyroid cancer and other malignancies. All other tests were exploratory. For classification, stratified 5-fold cross-validation (CV) was repeated 10 times with seeds 0–9. Splits were at the subject level and model settings were fixed. Only Synthetic Minority Over-sampling Technique (SMOTE) within training folds was used. Uncertainty for classification metrics was estimated by bootstrap resampling of out-of-fold predictions (Supplementary Table S5).

After QC, thyroid-cancer patients (n=81) had higher Band 1 energy than others (n=235). Mean±SD was 13.32±17.15 vs 10.12±21.52. Median [interquartile range (IQR)] was 9.23 [5.02–15.22] vs 6.23 [3.01–11.00]. The main group test was Mann–Whitney U (MW-U), with p = 0.0014. Cohen's d was 0.157 (Table 1). Both distributions are right-skewed, so medians were reported alongside means. It can be seen that the standardized effect is small and there is clear overlap between groups. The shift can still be seen across the full distribution (Fig. 2b), and it can also be seen under stricter QC settings (Fig. 2c). A robustness check after 1.5×IQR outlier removal (4 thyroid, 13 other) is reported. Under that rule, the effect estimate increases, with p < 0.001 and d = 0.530. The main claim does not depend on removing outliers. The recording site—finger and wrist—is far from the thyroid gland. If confirmed, the association is more likely systemic than organ-local.

Table1 Group comparison of Band 1 energy (0.025–0.2 Hz) between thyroid cancer and other cancers after automated QC exclusion (5 participants removed)

Group	Mean±SD	Median [IQR]	□ (MW-□)	Cohen's *d*
Thyroid (□=81)	13.32±17.15	9.23 [5.02–15.22]	0.0014	0.157
Other (□=235)	10.12±21.52	6.23 [3.01–11.00]		

After 1.5×IQR outlier removal (Thyroid n=77, Other n=222):
p (MW-*U*) < 0.001 Cohen's *d* = 0.530

Both parametric (Mean±SD) and non-parametric (Median [IQR]) descriptors are reported because Band 1 energy is right-skewed.

Depression risk (Patient Health Questionnaire-9 [PHQ-9] ⩾ 10) was also included as an exploratory analysis. Only BSP-derived signal features were used, and the same QC and CV rules were kept. Performance was near chance, with an area under the receiver operating characteristic curve (AUC) ≈ 0.50 (Supplementary Table S5). Band 1 does not independently separate depression-risk groups in this cohort. This null result helps to determine what the infra-slow features can and cannot do in this dataset.

Unedited

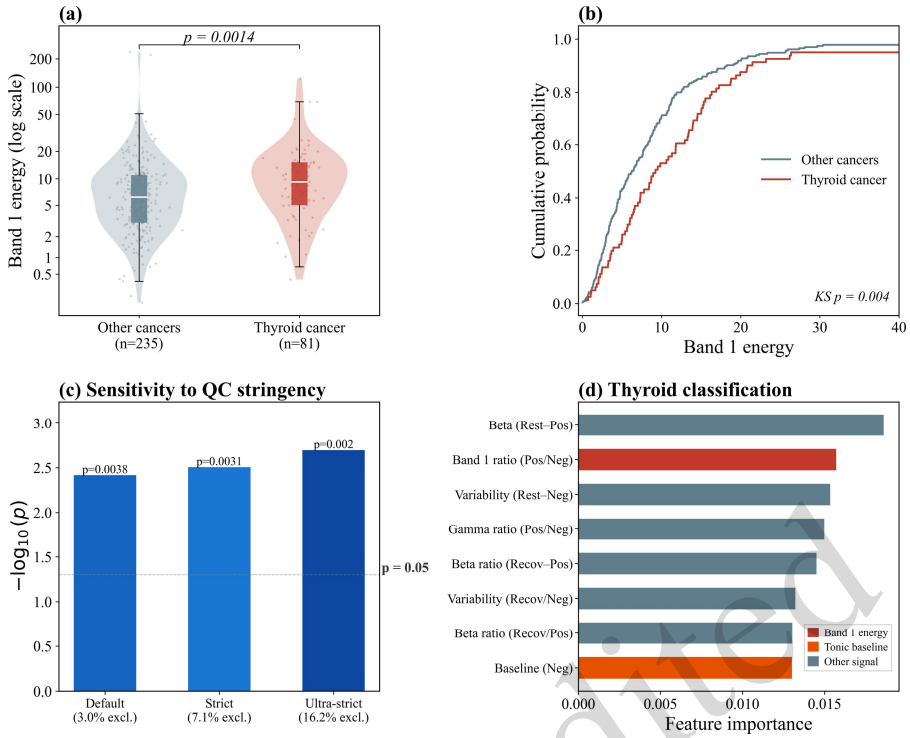

Fig. 2 Thyroid-cancer association in the low-frequency signal space (post-QC cohort, N = 316). (a) Violin plots with individual data points show elevated Band 1 energy (0.025–0.2 Hz) in thyroid cancer relative to other cancers (P = 0.0014, Mann–Whitney U). (b) Cumulative distribution functions confirm a distributional shift (Kolmogorov–Smirnov [KS] test, P = 0.004). (c) Sensitivity to QC stringency: the group difference persists under stricter artifact removal (all P < 0.005). (d) Feature-importance ranking for the thyroid-cancer classifier in this cohort.

Unedited

The above results suggest that infra-slow BSP features can act as a non-invasive marker of the systemic state in oncology. The main mechanism is simple: Band 1 energy from a short two-electrode recording remains detectable after QC and under stricter artifact removal. This effect is group-level and the distributions overlap. However, we do not claim diagnostic use in individuals. Signal-only classification is near-chance (Supplementary Table S5). A practical next step is to test whether Band 1 energy tracks endocrine or metabolic measures in thyroid disease. Another possible step is to test whether it is stable within a person across repeated sessions. Meanwhile, given these findings, the physiological source is not yet clear. The features may reflect electrodermal activity, blood flow, metabolism, medication, or other slow processes. Multi-modal recordings will be needed to separate these factors. Independent cohorts will also be necessary to validate the marker.

Despite the promising results, there are some limitations. First, the CTP008 lacks real-time impedance logging. The QC pipeline and sensitivity analysis may help compensate for this, but direct impedance monitoring would be better. Second, temperature and perspiration were not tracked. Third, we did not model key clinical covariates. Medication and pain are two examples, and both can affect autonomic state. Fourth, the single-center cohort has no healthy controls. Multi-site replication with standardized placement and a healthy reference group is needed (Zhang et al., 2024). Test–retest reliability and device calibration also remain to be analyzed and performed. A direct next step would be independent replication with DC-coupled hardware and shared analysis code.

Materials and methods

Detailed methods are provided in the electronic supplementary materials of this paper.

Data availability statement

The datasets generated and/or analyzed during the current study are available from the corresponding author on reasonable request. The data are not publicly available due to privacy restrictions and ethical considerations regarding patient information.

Acknowledgments

This work was supported by the 2025 Beilun District Health Science and Technology Plan Project (No. 2025BLWSZD001) and the Shenzhen Basic Research Program of Natural Science Foundation (No. JCYJ20250604185425033). We thank all the patients who participated in this study and the medical staff at The First Affiliated Hospital of Zhejiang University School of Medicine for their assistance in data collection.

Author contributions

Bohan DENG designed the study, developed the software, performed the formal analysis, curated the data, wrote the original draft, and created the visualizations. Ruili ZHANG contributed to methodology development, validation, investigation, and data curation. Yuxuan LIU participated in formal analysis. Jinglao LIN contributed to software development and formal analysis. Shicong GUI contributed to software development and visualization. Xihao WEI contributed to visualization. Yin CHENG contributed to validation and investigation. Li ZHENG contributed to validation. Shaohua HU contributed to the study conceptualization. Pingping LYU contributed to validation and investigation. Yubo LI conceptualized the study, provided resources, reviewed and edited the manuscript, supervised the project, and acquired funding. Huafen WANG conceptualized the study, provided resources, reviewed and edited the manuscript, supervised the project, and acquired funding. All authors have read, approved the final manuscript, and share responsibility for the publication.

Unedited

Compliance with ethics guidelines

Conflict of interest: Bohan DENG, Ruili ZHANG, Yuxuan LIU, Jinglao LIN, Shicong GUI, Xihao WEI, Yin CHENG, Li ZHENG, Shaohua HU, Pingping LYU, Yubo LI, and Huafen WANG declare that they have no conflict of interest.

Ethics statement: This study was conducted in accordance with the ethical principles of the World Medical Association Declaration of Helsinki. The protocol was approved by the Institutional Review Board of The First Affiliated Hospital of Zhejiang University School of Medicine (approval No. IIT20250462B). Written informed consent was obtained from all participants before enrollment. All participant data were anonymized throughout the study to ensure confidentiality.

Consent to publish: Not applicable because no identifiable individual data are included in this manuscript.

Declaration on the use of generative AI tools

During the preparation of this work, the authors used an AI coding assistant (powered by Large Language Models) in order to improve language and readability and assist with LATEX formatting. After using this tool/service, the authors reviewed and edited the content as needed and take full responsibility for the content of the publication.

References

Boucsein, W. (2012). Electrodermal Activity (2nd ed.). Springer, New York. https://doi.org/10.1007/978-1-4614-1126-0

Hammond, N. G., Cameron, R. B., & Faubert, B. (2024). Beyond glucose and Warburg: finding the sweet spot in cancer metabolism models. NPJ Metabolic Health and Disease, 2(1), 11. https://doi.org/10.1038/s44324-024-00011-0

Lyu, H., Huang, H. M., He, J. D., Zhu, S., Hong, W. C., Lai, J. B., & Hu, S. H. (2024). Task-state skin potential abnormalities can distinguish major depressive disorder and bipolar depression from healthy controls. Translational Psychiatry, 14(1), 8. https://doi.org/10.1038/s41398-023-02710-y

Posada-Quintero, H. F., & Chon, K. H. (2020). Innovations in electrodermal activity data collection and signal processing: a systematic review. Sensors, 20(2), 479. https://doi.org/10.3390/s20020479

Zhang, L., Xing, S. C., Yin, H. F., Weisbecker, H., Tran, H. T., Guo, Z. H., Han, T., Wang, Y., Song, Y. M., Zhu, W. Q., Xu, K. C., & Lu, N. S. (2024). Skin-inspired, sensory robots for electronic implants. Nature Communications, 15(1), 4777. https://doi.org/10.1038/s41467-024-49131-1

Supplementary information:

Included supplementary materials are Materials and methods and Supplementary Tables S1–S5. All supplementary materials are cited in the main text.

Unedited